

Electronic properties of silole-based organic semiconductors

C. Risko, G. P. Kushto, Z. H. Kafati, and J. L. Brédas

Citation: *J. Chem. Phys.* **121**, 9031 (2004); doi: 10.1063/1.1804155

View online: <http://dx.doi.org/10.1063/1.1804155>

View Table of Contents: <http://jcp.aip.org/resource/1/JCPSA6/v121/i18>

Published by the [American Institute of Physics](#).

Additional information on *J. Chem. Phys.*

Journal Homepage: <http://jcp.aip.org/>

Journal Information: http://jcp.aip.org/about/about_the_journal

Top downloads: http://jcp.aip.org/features/most_downloaded

Information for Authors: <http://jcp.aip.org/authors>

ADVERTISEMENT



**ALL THE PHYSICS
OUTSIDE OF
YOUR JOURNALS.**

www.physics today.org
**physics
today**

Electronic properties of silole-based organic semiconductors

C. Risko

School of Chemistry and Biochemistry, Georgia Institute of Technology, Atlanta, Georgia 30332-0400

G. P. Kushto and Z. H. Kafati

Optical Sciences Division, US Naval Research Laboratory, Washington, DC 20375

J. L. Brédas

School of Chemistry and Biochemistry, Georgia Institute of Technology, Atlanta, Georgia 30332-0400

(Received 23 April 2004; accepted 16 August 2004)

We report on a detailed quantum-chemical study of the geometric structure and electronic properties of 2,5-bis(6'-(2',2''-bipyridyl))-1,1-dimethyl-3,4-diphenylsilole (*PyPySPyPy*) and 2,5-di-(3-biphenyl)-1,1-dimethyl-3,4-diphenylsilole (*PPSPP*). These molecular systems are attractive candidates for application as electron-transport materials in organic light-emitting devices. Density Functional Theory (DFT), time-dependent DFT, and correlated semiempirical (ZINDO/CIS) calculations are carried out in order to evaluate parameters determining electron-transport and optical characteristics. Experimental data show that *PyPySPyPy* possesses an electron-transport mobility that is significantly greater than *PPSPP*, while *PPSPP* has a significantly larger photoluminescence quantum yield; however, the theoretical results indicate that the two systems undergo similar geometric transformations upon reduction and have comparable molecular orbital structures and energies. This suggests that intermolecular interactions (solid-state packing, electronic coupling) play significant roles in the contrasting performance of these two molecular systems. © 2004 American Institute of Physics. [DOI: 10.1063/1.1804155]

I. INTRODUCTION

The development of organic molecular and polymeric systems for use as semiconducting materials in electronic, optoelectronic, and electro-optic devices has brought forth a number of remarkable discoveries,^{1,2} and has led to their recent commercialization in consumer products.³ The continued emergence of these new technologies will rely heavily upon performance enhancement in such matters as charge injection and transport efficiency, photoluminescence quantum yields, and temporal and thermal stability. Silole (silacyclopentadiene)-based systems have recently garnered much attention as electron-transport materials due to the presence of a low-lying lowest unoccupied molecular orbital (LUMO).⁴ The σ^* - π^* conjugation in the ring due to interaction between the σ^* orbitals of the two exocyclic silicon-carbon bonds with the π^* orbital of the butadiene moiety provides the stable features of the LUMO level.⁵ The low-lying LUMO provides silole-based systems with large electron affinities coupled with redox stability in air.⁴⁻⁷ These intrinsic characteristics have led to very high electron mobilities, and in some cases nondispersive and air-stable electron transport. For instance, 2,5-bis(6'-(2',2''-bipyridyl))-1,1-dimethyl-3,4-diphenylsilole (*PyPySPyPy*) exhibits very high, nondispersive, air-stable time-of-flight electron mobility of 2×10^{-4} cm²/Vs, a two-order of magnitude improvement compared to the well-established electron transporter tris(quinolin-8-olato) aluminum(III) (Alq₃).^{6,7}

Recent studies on organic light-emitting diodes based on *PyPySPyPy* and its biphenyl analog 2,5-di-(3-biphenyl)-1,1-dimethyl-3,4-diphenylsilole (*PPSPP*), see Fig. 1, have

demonstrated that these two chemically similar molecular systems display distinctly different solid-state properties. Polycrystalline films of *PyPySPyPy* and *PPSPP* display green (2.46 eV) and blue (2.61 eV) fluorescence with absolute photoluminescence (PL) quantum yields of $28\% \pm 3\%$ and $85\% \pm 5\%$, respectively.^{8,9} The PL quantum yield for *PPSPP* is among the highest reported for neat organic films.^{7,8} We note that Chen *et al.*¹⁰ have reported the appearance of the phenomenon of aggregation-induced emission for 1,1-dimethyl-2,3,4,5-tetraphenylsilole (*PSP*), a smaller analog of *PPSPP*. In addition, two-layer films of *PPSPP* or *PyPySPyPy* with the hole-transport material *N,N'*-diphenyl-*N,N'*-(2-naphthyl)-(1,1'-phenyl)-4,4'-diamine (*NPB*) show exciplex PL quantum yields of 62% (*PPSPP*) and 21% (*PyPySPyPy*). The *NPB:PPSPP* exciplex PL quantum yield is the highest reported to date.⁸ As for their use as electron-transport materials, single-layer electron-only devices fabricated using *PyPySPyPy* exhibit a higher current flow than devices made using *PPSPP*. This suggests that *PyPySPyPy* has higher electron conductivity signifying both higher electron mobility and a lower barrier to electron injection than *PPSPP*.^{8,11}

The purpose of the present work is to determine theoretically the electronic structures of *PyPySPyPy* and *PPSPP* in order to understand the chemical and physical properties that control their remarkably distinctive thin-film electronic properties. We use Density Functional Theory and correlated semiempirical methods to describe the geometric and electronic structures and optical properties of these molecules. Here, our focus will be on the geometric structures of both

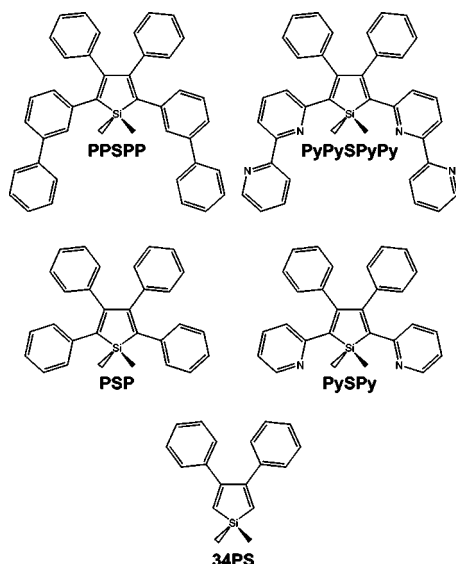


FIG. 1. Chemical structures of: 1,1-dimethyl-3,4-diphenylsilole (34PS), 1,1-dimethyl-2,5-bis(2'-pyridyl)-3,4-diphenylsilole (*PySPy*), 1,1-dimethyl-2,3,4,5-tetraphenylsilole (*PSP*), 2,5-bis(6'-(2',2''-bipyridyl))-1,1-dimethyl-3,4-diphenylsilole (*PyPySPyPy*), and 2,5-di-(3-biphenyl)-1,1-dimethyl-3,4-diphenylsilole (*PPSPP*).

the neutral molecules and their radical-anions, the absorption spectra of the neutral species, and the evaluation of the intramolecular reorganization energies and electron affinities of *PyPySPyPy* and *PPSPP*.

II. THEORETICAL METHODOLOGY

In order to better understand the geometric and electronic structure of the relatively large molecular systems *PyPySPyPy* and *PPSPP*, we have assessed also their constitutive molecular fragments so as to build a complete picture of the roles of the numerous intramolecular interactions. In that context, we have considered the molecules 1,1-dimethyl-3,4-diphenylsilole (34PS), 1,1-dimethyl-2,5-bis(2'-pyridyl)-3,4-diphenylsilole (*PySPy*), and 1,1-dimethyl-

2,3,4,5-tetraphenylsilole (*PSP*) in addition to *PyPySPyPy* and *PPSPP* (see Fig. 1). The geometries were optimized in two different electronic configurations corresponding to the neutral and reduced radical-anion states. For the sake of completeness, the neutral states of pyridine, benzene, bipyridine, and biphenyl were also investigated.

The geometry optimizations were carried out at the Density Functional Theory (DFT) level using the B3LYP functionals, where Becke's three-parameter hybrid exchange functional is combined with the Lee–Yang–Parr correlation functional,^{12,13} and a 6-31G* split valence plus polarization basis set. The size of the larger molecular systems limited the basis set from extension with diffuse functions; such basis functions, which are generally prescribed for the proper description of small molecular anions,^{14,15} proved either to be computationally expensive or not to allow convergence of the iterative procedures. As a result, the energetic values of the anionic systems will only be used here to provide relative values of the intramolecular reorganization energy and the electron affinity. The excitation energies of the low-lying excited states have been calculated at the time-dependent DFT (TDDFT) level and with Zerner's semiempirical intermediate neglect of differential overlap (ZINDO) (Ref. 16) method supplemented by a single-configuration interaction (CIS) scheme. All DFT calculations were carried out with the GAUSSIAN98 suite of programs.¹⁷

III. RESULTS AND DISCUSSION

A. Geometry

The DFT optimized geometries are collected in Tables I and II, using the bond numbering scheme presented in Fig. 2. In all instances, the silole ring is found to be nearly coplanar with maximum deviations from planarity on the order of 4°. In 34PS, see Table I, the exocyclic carbon-silicon bonds (1.893 Å) are slightly longer than the in-ring carbon-silicon bonds (1.875 Å). The *cis*-butadiene portion of the silole ring presents a very large degree of bond-length alternation

TABLE I. B3LYP/6-31G*-optimized bond lengths (Angstroms) for the neutral and anionic electronic configurations of 34PS, *PyPySPyPy*, and *PPSPP* (see Fig. 2 for bond numbering). Δ (Anion-Neutral) values are provided for each system.

Bond	34PS			<i>PyPySPyPy</i>			<i>PPSPP</i>		
	Neutral	Anion	Δ	Neutral	Anion	Δ	Neutral	Anion	Δ
1	1.893	1.923	0.030	1.888	1.903	0.015	1.893	1.912	0.019
2	1.893	1.923	0.030	1.888	1.903	0.015	1.893	1.911	0.018
3	1.875	1.846	-0.029	1.892	1.879	-0.013	1.886	1.871	-0.015
4	1.875	1.846	-0.029	1.892	1.879	-0.013	1.886	1.870	-0.016
5	1.357	1.402	0.045	1.367	1.414	0.047	1.367	1.415	0.048
6	1.357	1.402	0.045	1.367	1.414	0.047	1.367	1.415	0.048
7	1.520	1.474	-0.046	1.509	1.452	-0.057	1.513	1.456	-0.057
8	1.487	1.472	-0.015	1.493	1.490	-0.003	1.493	1.487	-0.006
9	1.487	1.472	-0.015	1.493	1.490	-0.003	1.493	1.487	-0.006
10	1.473	1.443	-0.030	1.479	1.457	-0.022
11	1.410	1.430	0.020	1.408	1.423	0.015
12	1.351	1.369	0.018	1.406	1.420	0.014
13	1.473	1.443	-0.030	1.479	1.457	-0.022
14	1.410	1.430	0.020	1.408	1.423	0.015
15	1.351	1.369	0.018	1.406	1.420	0.014

TABLE II. Selected bond lengths (Angstroms) for the neutral and anionic electronic configurations of *PySPy* and *PSP* (see Fig. 2 for bond numbering). In addition to the B3LYP/6-31G* results from this work, in the case of *PSP*, we also list the bond lengths obtained via x-ray diffraction (Ref. 21) and HF-AM1 calculations (Ref. 20). Δ (Anion-Neutral) values are also provided for each system at the DFT level of theory.

Bond	PySPy			PSP				
	Neutral	Anion	Δ	Neutral			Anion	Δ
	B3LYP/6-31G*	B3LYP/6-31G*		Experiment ^a	AM1 ^b	B3LYP/6-31G*	B3LYP/6-31G*	
1	1.887	1.901	0.014	1.86	1.818	1.893	1.914	0.021
2	1.887	1.901	0.014	1.86	1.818	1.893	1.914	0.021
3	1.896	1.881	-0.015	1.87	1.833	1.886	1.869	-0.017
4	1.896	1.881	-0.015	1.87	1.833	1.886	1.869	-0.017
5	1.368	1.414	0.046	1.36	1.353	1.367	1.416	0.049
6	1.368	1.414	0.046	1.36	1.353	1.367	1.416	0.049
7	1.507	1.453	-0.054	1.51	1.486	1.513	1.456	-0.057
8	1.494	1.490	-0.004	1.49	...	1.492	1.487	-0.005
9	1.494	1.490	-0.004	1.49	...	1.492	1.487	-0.005
10	1.469	1.440	-0.029	1.48	...	1.479	1.458	-0.021
11	1.411	1.429	0.018	1.408	1.422	0.014
12	1.357	1.376	0.019	1.409	1.422	0.013
13	1.469	1.440	-0.029	1.48	...	1.479	1.458	-0.021
14	1.411	1.429	0.028	1.409	1.422	0.013
15	1.357	1.376	0.019	1.408	1.422	0.014

^aSee Ref. 17.

^bSee Ref. 16.

(BLA) between the single and double carbon-carbon bonds, on the order of 0.163 Å; the single bond is especially long (1.520 Å) for a conjugated system, which is likely a consequence of the steric interactions between the phenyl rings attached at the 3- and 4-positions. The phenyl groups attached at the 3- and 4-positions have carbon-carbon bridge bond lengths of 1.487 Å; the rings, rotated in-phase, lay $\sim 45^\circ$ out-of-plane with respect to the silole ring. We note that the results obtained for the silole ring are in good agreement with previous computational analyses of silole systems performed at the B3LYP/6-31G*(C,H)/LanL2DZdp(Si),¹⁸ HF/66-31G*(Si)/6-31G*(C)/31G*(H),¹⁹ HF/6-31G*,⁵ and HF-AM1 (Ref. 20) levels of theory.

Extending the *34PS* system by addition of either pyridyl (*PySPy*) or phenyl (*PSP*) groups at the 2- and 5-positions only slightly alters the overall geometry of the silole core, see Table II. Both *PySPy* and *PSP* maintain exocyclic carbon-silicon bond lengths of 1.89 Å; however, the in-ring carbon-silicon bonds differ by 0.01–0.02 Å for *PySPy*

(1.896 Å) and *PSP* (1.886 Å). The BLA parameter, though somewhat smaller than in *34PS*, remains large (0.139 Å in *PySPy* and 0.146 Å in *PSP*); the difference in BLA between the two systems is due to a slightly shorter single bond in the *cis*-butadiene moiety for *PySPy*. The phenyl rings at the 3- and 4-positions acquire more significant torsions for both *PySPy* ($\sim 70^\circ$) and *PSP* ($\sim 57^\circ$) with bridge bond lengths of 1.49 Å. Interestingly, rather pronounced geometric differences are found at the 2- and 5-aryl substitutions: the pyridyl rings in *PySPy* lay relatively in-plane with the silole ring ($\sim 18^\circ$) while the phenyl rings of *PSP* are rotated by some 50° ; in addition, the carbon-carbon bridge bond length is 0.01 Å shorter for *PySPy*. The geometric distortions in *PSP* are likely related to the hydrogen present at the 2-position on the phenyl ring that imparts steric interactions with the silicon-substituted methyl groups and, thus, prevents the more planar structure observed for the pyridyl substituents.

The optimized geometric parameters at the B3LYP/6-31G* level for *PSP* are in good agreement with the reported x-ray crystal structure determination of Párkányi.²¹ The exocyclic silicon-carbon bonds are slightly overestimated (0.03 Å), while the in-ring silicon-carbon bonds are underestimated (0.02 Å). Excellent agreement is found for the carbon-carbon bonds within the *cis*-butadiene moiety and, hence, for the degree of BLA. It is of note that the experimental BLA (0.15 Å) of the *cis*-butadiene segment in *PSP* is larger than that observed for a similar silole system that is hydrogen-substituted at the 3- and 4-positions (0.12 Å);²¹ thus, this confirms that relaxation of the steric interactions of the phenyl substituents is achieved through a lengthening of the bonds in the *cis*-butadiene fragment. Additionally, the mean torsional angles of the phenyl groups found in the x-ray structure at both the 3- and 4-positions

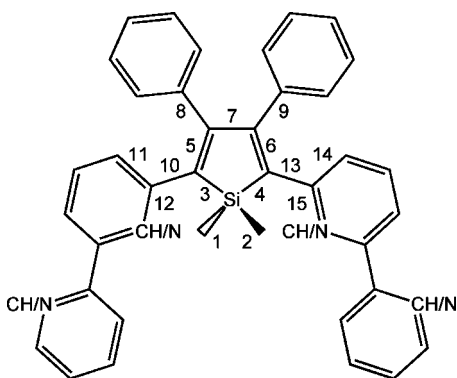


FIG. 2. Bond numbering scheme used for *34PS*, *PySPy*, *PSP*, *PyPySPyPy*, and *PPSP*.

($\sim 58^\circ$) and 2- and 5-positions ($\sim 45^\circ$) are well reproduced by the DFT optimizations.

No significant modifications to the silole unit are incurred upon addition of the external aryl rings for *PyPySPyPy* and *PPSPP*, see Table I. For the respective larger analogs, the BLA of the *cis*-butadiene segment, as well as the bond lengths and torsion angles of the phenyl substituents at the 3- and 4-positions, are preserved. The substitutions at the 2- and 5-positions for both *PyPySPyPy* and *PPSPP* maintain the bridging bond lengths of *PySPy* and *PSP*, respectively. However, the torsion angle in *PyPySPyPy* (32°) does increase somewhat versus the smaller analog ($\sim 18^\circ$); there is virtually no difference between *PPSPP* and *PSP*. Note that the lowest energy conformer for *PyPySPyPy* is that with the nitrogen atoms of each bipyridyl unit in a *trans*-conformation (the *cis*-conformation is calculated at the DFT level to be 9.6 kcal/mol higher in energy). The torsion angles within the bipyridyl and biphenyl substituents are $\sim 7^\circ$ and $\sim 37^\circ$, respectively. We note that the DFT-calculated dipole moments for *PPSPP* and *PyPySPyPy* are both very small: *PPSPP* has a dipole moment of 0.26 D in the *syn*-conformation, while the presence of the nitrogen atoms in the pyridine rings makes the molecular dipole of *PyPySPyPy* somewhat larger (0.59 D).

Upon reduction to the radical-anion state, the modifications in geometry of the considered molecules are primarily confined to the silole ring and the aryl rings directly bound at the 2- and 5-positions on the silole ring. In *34PS*, the silicon-carbon bonds relax rather considerably with the exocyclic bonds lengthening by 0.03 Å and the in-ring silicon-carbon bonds shortening by the same extent (0.03 Å). These changes in bond length are related to the fact that reduction to the radical-anion populates the silole LUMO; this population allows for increased antibonding (σ^*) interaction between the silicon and exocyclic methyl carbons that lengthens these bonds, while bringing forth increased bonding character for the in-ring silicon-carbon bonds through the extended conjugation provided by the interaction of the low-lying silicon p_z orbital and the π^* orbital of the *cis*-butadiene unit. Population of the LUMO also causes a dramatic decrease by half in the BLA of the *cis*-butadiene moiety; the respective double bonds lengthen by 0.045 Å and the single bond shortens by 0.046 Å. The phenyl rings at the 3- and 4-positions maintain rather similar torsion angles ($\sim 35^\circ$) and bridging carbon-carbon bond lengths (1.472 Å).

The nature of the changes in the silicon-carbon bonds for *PySPy* and *PSP*, though smaller in absolute terms, are similar to those observed for *34PS* upon reduction. The lesser extent of the silicon-carbon bond length modifications is linked to a delocalization of the radical-anion to the aryl rings at the 2- and 5-positions. The *cis*-butadiene portions of the two systems, as well, undergo similar transformations: for *PySPy* (*PSP*), the double bonds increase by 0.046 (0.049) Å while the single bond decreases by 0.054 (0.057) Å; these changes produce a BLA of 0.039 (0.040) Å, a decrease of over 70%. While some change occurs to the torsion angles of the phenyl groups substituted at the 3- and 4-positions in *34PS*, there are no marked changes in either

PySPy or *PSP*. The 2- and 5-position pyridyl substituents in *PySPy* undergo a slight increase in the planarity with the silole ring as the torsion angles decrease from 18° to $\sim 10^\circ$. The bridging carbon-carbon bond decreases by 0.029 Å while the adjacent carbon-carbon and carbon-nitrogen bonds increase by ~ 0.018 Å; thus, as was seen in the *cis*-butadiene portion of the silole ring, a loss of BLA is continued throughout this portion of the molecular system. Similar types of bond transformations at the 2- and 5-phenyl substitutions are observed for *PSP* as well. The bridging bond decreases (0.021 Å), while the first carbon-carbon bonds within the ring increase (0.013–0.014 Å). However, there is a much more drastic shift towards planarity for this system as the torsion angle at the 2- and 5-positions shifts from 45° to 23° .

Parallel geometric transformations to those for *PySPy* and *PSP* are observed upon reduction of *PyPySPyPy* and *PPSPP*, respectively. For instance, within the *cis*-butadiene moiety, the BLA decreases to 0.038 Å for *PyPySPyPy* and 0.041 Å for *PPSPP*; a loss of BLA in the bonds in immediate proximity to the 2- and 5-positions on the silole ring occurs also in both *PyPySPyPy* and *PPSPP* (we note that the remaining bonds in both the bipyridyl and biphenyl units change by <0.01 Å). The main distinction between the two radical-anion structures is the relative planarity between the silole ring and the bipyridyl or biphenyl units. The bipyridyl units in *PyPySPyPy* (23°) become more coplanar with respect to the silole ring; also, the dihedral distortions between the pyridine segments are virtually negligible (1.3°). The biphenyl units in *PPSPP* undergo slightly larger torsional shifts from 50° in the neutral state to 37° in the radical-anion state, while the torsions between the phenyl rings change by only 2° . Overall, we observe that the geometry relaxations upon reduction are confined to the silole ring and the parts adjacent to it of the aryl rings substituting in the 2- and 5-positions.

B. Electronic structure and optical absorption

Though *PySPy* and *PyPySPyPy* have similar absorption maxima (3.37 eV and 3.28 eV, respectively), the two molecules possess rather different solid-state properties: *PySPy* is crystalline, while *PyPySPyPy* is amorphous with a glass transition temperature T_g of 77°C .²² Based on these observations, Uchida *et al.*²² suggested that the addition of the extra aryl groups simply serve as a means to add more flexibility to *PyPySPyPy* while having minimal effect on the HOMO (highest occupied molecular orbital)-LUMO (lowest unoccupied molecular orbital) gap.²²

To better understand the optical data, we now turn to a description of the main characteristics of the HOMO and LUMO levels, as calculated at the DFT level. Analysis of the HOMO wave function for *34PS* (-5.68 eV) indicates that it mainly resides on the *cis*-butadiene moiety; its bonding-antibonding pattern is consistent with observations in the geometrical analysis of the neutral species, see Fig. 3. Aryl substitution at the 2- and 5-positions to form *PySPy* and *PSP* brings forth electronic interactions between the HOMO of *34PS* and the highest π orbitals of pyridine (-7.11 eV) and benzene (-6.70 eV). Because the highest π orbitals for *34PS* and benzene are closer in energy than *34PS* and pyri-

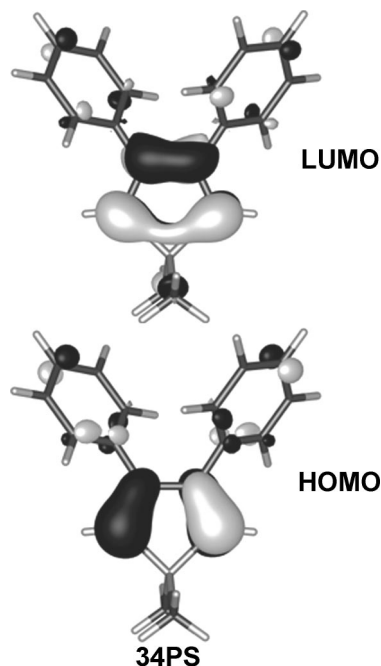


FIG. 3. B3LYP/6-31G*—calculated highest occupied (HOMO) (bottom) and lowest unoccupied (LUMO) (top) one-electron molecular orbitals for 34PS.

dine, a larger energy destabilization is expected *a priori* for the *PSP* HOMO through a greater degree of orbital splitting produced by more pronounced wave function overlap. However, the HOMO energies for *PySPy* (−5.28 eV) and *PSP* (−5.29 eV), are nearly identical. This is due, at least partly, to the more planar structure of *PySPy* which allows for a greater degree of antibonding orbital interaction (see below) than the more twisted structure of *PSP*. Examination of the wave functions shows that their spatial distributions are very similar in the two systems, see Fig. 4; they primarily lie on the silole ring and the aryl rings substituted at the 2- and 5-positions with an antibonding character between the silole ring and the respective aryl substituent.

Addition of external aryl groups in *PyPySPyPy* and *PPSPP* again produces HOMO levels that have nearly identical energies, −5.33 and −5.32 eV, respectively. This is in excellent agreement with the ultraviolet-photoelectron spectroscopy (UPS) experimental data that indicate that the solid-

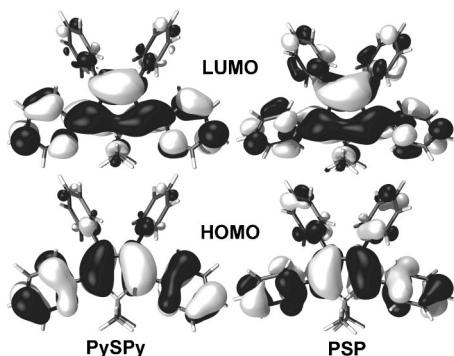


FIG. 4. B3LYP/6-31G*—calculated highest occupied (HOMO) (bottom) and lowest unoccupied (LUMO) (top) one-electron molecular orbitals for *PySPy* (left) and *PSP* (right).

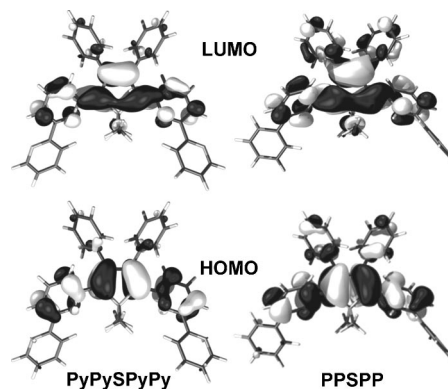


FIG. 5. B3LYP/6-31G*—calculated highest occupied (HOMO) (bottom) and lowest unoccupied (LUMO) (top) one-electron molecular orbitals for *PyPySPyPy* (left) and *PPSPP* (right).

state ionization potentials of *PyPySPyPy* and *PPSPP* differ by only 0.05 eV (5.94 and 5.89 eV, respectively).^{8,23,24} As with their smaller analogs, the orbital distributions are nearly identical for the two systems with the majority of the probability density residing on the silole ring and the aryl rings substituted at the 2- and 5-positions, see Fig. 5. In fact, the HOMO's for the *PySPy/PyPySPyPy* and *PSP/PPSPP* pairs are virtually indistinguishable (neglecting the small amount of orbital density on the external aryl rings of the larger systems).

The DFT B3LYP/6-31G* calculations indicate that the LUMO for 34PS lies at −1.37 eV; as with the HOMO, it resides primarily on the silole ring. The LUMO shape maintains the primary characteristics of the isolated silole ring in which interaction between the σ^* orbitals of the two exocyclic σ bonds on the ring silicon and the π^* orbital of the butadiene moiety composes the σ^* - π^* conjugation in the ring, see Fig. 3. Addition of pyridyl and phenyl at the 2- and 5-positions to form *PySPy* and *PSP* produces LUMO energies of −1.82 and −1.59 eV, respectively (note that the pyridine LUMO is calculated to lie at −0.68 eV, while that of benzene at 0.10 eV). The wave functions are very similar for the two systems, see Fig. 4, and are primarily located on the silole ring and the aryl rings substituted at the 2- and 5-positions with a bonding character between the silole ring and the substituent. Further extension with outer aryl groups in *PyPySPyPy* and *PPSPP* produces LUMO levels at −1.84 and −1.63 eV, respectively. Though the DFT LUMO energy results slightly overestimate the difference in the solid-state LUMO levels of *PyPySPyPy* and *PPSPP* (0.06 eV) as determined by the combination of UPS and optical-band gap data,^{8,23,24} there is concurrence with the fact that the LUMO for *PyPySPyPy* is energy stabilized versus *PPSPP*. Again, the orbital distributions are nearly identical for the two systems with the majority of the probability density residing on the silole ring and the aryl rings substituted at the 2- and 5-positions, see Fig. 5. As with the HOMO wave functions, the LUMO wave functions of the larger systems are virtually indistinguishable from the smaller molecules. The ~0.2 eV stabilization in the LUMO energy for *PyPySPyPy* versus *PPSPP* could be one of the main fac-

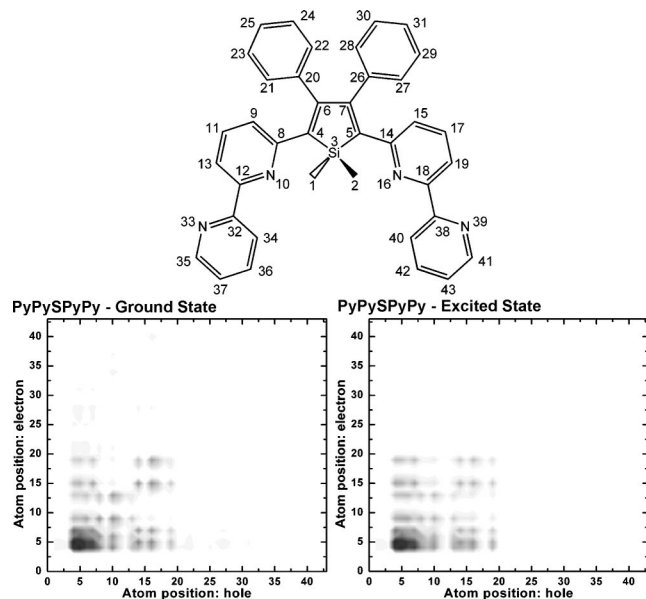


FIG. 6. Electron-hole distributions and atomic labeling scheme for *PySPy* (ground state geometry) and *PyPySPyPy* (ground and excited state geometries).

tors in the electron transport differences of the two molecular systems.

PyPySPyPy and *PySPy* photoluminesce at 2.53 and 2.58 eV in THF after absorption with maxima at 3.28 and 3.37 eV, respectively.²² The photoluminescence and absorption wavelengths vary only slightly for the two materials in thin films with values of 2.50 and 3.21 eV for *PyPySPyPy* and 2.54 and 3.26 eV for *PySPy*.²² The INDO/CIS evaluation of the absorption energies for *PyPySPyPy* (3.50 eV) and *PySPy* (3.48 eV) are in very good agreement with the experimental data and confirm the similarity in the absorption maxima; the INDO/CIS emission energies, calculated on the basis of AM1/CI-optimized geometries of the lowest excited state,²⁵ are also in good agreement with experiment (2.88 eV for *PyPySPyPy* and 2.80 eV for *PySPy*). Optical data¹⁷ for *PSP* indicates that the system undergoes intense fluorescence in the blue region of the visible spectrum (2.58 eV) after absorption with a maximum at 3.53 eV. INDO/CIS calculations for *PSP* absorption (3.78 eV) show good agreement with the empirical absorption maximum; the calculated absorption maximum for *PPSPP* is 3.78 eV, as well; the calculated emission energies are 3.07 and 3.01 eV for *PPSPP* and *PSP*, respectively. TDDFT results for the absorption maxima of *PyPySPyPy* (3.07 eV) and *PPSPP* (3.20 eV) are in good agreement with the INDO/CIS results.

Evaluation of the nature of the excited state through investigation of electron-hole distribution²⁶ for *PyPySPyPy*, see Fig. 6, reveals that the exciton is predominantly located on the silole ring and the pyridine rings directly substituted at the 2- and 5-positions. Very similar electron-hole distributions are evaluated for *PySPy*, *PSP*, and *PPSPP* and are thus not shown here. These results indicate that (i) the addition of the external aryl ring does not affect the location of the exciton, which is consistent with the molecular orbital analysis, and (ii) as a consequence, the electron-hole distri-

butions are similar, whether taking account of the ground-state geometry or the lowest excited-state geometry;²⁶ this contrasts with the situation in well-conjugated oligomers, for instance, oligophenylenevinyls,²⁷ where the exciton wave function is initially significantly delocalized (ground-state geometry) but localizes upon nuclear relaxation (excited-state geometry).

The above quantum-chemical assessments of the orbital energies, orbital shapes, absorption data, and electron-hole distributions confirm the suggestion of Uchida *et al.*²² The addition of the aryl ring to *PySPy* to form *PyPySPyPy* has no significant effect on the HOMO-LUMO gap (3.46 eV and 3.49 eV, respectively) or on the electron-hole distribution. This is made even clearer by the fact that the calculated transitions for the two systems primarily involve a HOMO→LUMO transition (on the order of 88% and 83%, respectively). The calculated values for *PSP* and *PPSPP* are very similar; as a result, analogous absorption characteristics are predicted for these systems.

C. Intramolecular reorganization energy and electron affinity

When considering the transport properties of negative polarons as charge carriers through an organic molecular film, the electron-hopping process can be portrayed at the microscopic level as a self-exchange electron-transfer reaction between two neighboring molecules—the acceptor being in the neutral electronic state and the donor in the reduced radical-anion state. A simple analysis of such an electron-transfer reaction can be based on Marcus theory and extensions thereof,^{28,29} as done for instance in our earlier work.³⁰ In the context of Marcus theory, the rate constant for electron transfer (polaron hopping) can be defined in an Arrhenius-like manner:^{28,29}

$$k_{ET} = \frac{4\pi}{h} \frac{1}{\sqrt{4\pi\lambda k_B T}} t^2 \exp\left[\frac{-\lambda}{4k_B T}\right], \quad (1)$$

where t is the transfer integral (or electronic coupling matrix element) between neighboring molecules, λ the reorganization energy required during the intermolecular transfer of an electron, k_B the Boltzmann constant, and T the temperature. Quantum-chemical calculations allow for the description of both the transfer integral and the intramolecular reorganization energy.

The transfer integral is related to the energetic splitting of the frontier orbitals of the molecules as the system goes from isolated molecules to interacting molecules.³¹ In the absence of structural data for the relative positions of *PyPySPyPy* or *PPSPP* molecules in films, only exploratory evaluations of the transfer integrals can be performed. Analysis at the INDO level of theory of the intermolecular electronic coupling between dimers (with intermolecular distances ranging between 5 and 7 Å and variations in orientation) composed of molecules using the DFT-derived geometries indicates the following:

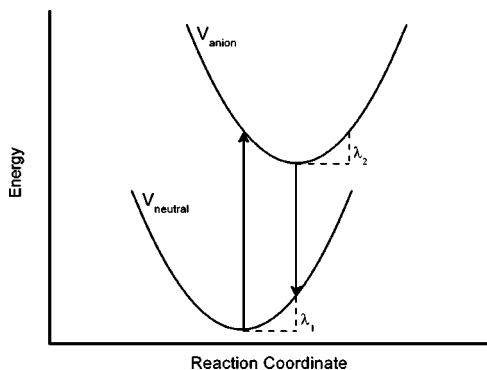


FIG. 7. Sketch of the potential energies of neutral (V_{neutral}) and anionic (V_{anion}) species, illustrating the neutral (λ_1) and anion (λ_2) relaxation energies.

(i) The more planar structure of *PyPySPyPy* appears to allow for shorter intermolecular distances and confirms the potential for larger transfer integrals versus *PPSPP*.

(ii) The transfer integrals for both electrons and holes are in the range of 10^{-2} – 10^{-3} eV; these results are one to two orders of magnitude lower than in ordered systems, such as crystalline pentacene.³²

The reorganization energy λ can be separated into the sum of two primary components: (i) the medium solvent reorganization energy which arises from modifications to the medium polarization due to the presence of excess charge; and (ii) the intramolecular reorganization energy, which combines the relaxation energies of the electron-donor (initially ionized) molecule λ_1 and of the electron-acceptor (initially neutral) molecule λ_2 , see Fig. 7, upon electron-transfer reaction.³³ Our goal here is to assess the extent of intramolecular reorganization energy in the silole-based systems. From Eq. (1), it is clear that for electron transfer (carrier hopping) rates to be high, reorganization energies need to be kept as low as possible.

The calculated intramolecular reorganization energies, see Table III, for *PyPySPyPy* (0.50 eV) and *PPSPP* (0.52 eV) demonstrate that the two systems, again, are very similar in nature. The slightly larger reorganization energy in *PPSPP* is consistent with the fact that while both *PyPySPyPy* and *PPSPP* undergo similar bond length changes upon reduction, *PPSPP* displays slightly larger torsional modifications. However, the major result is that the intramolecular reorganization energy values, ~ 0.5 eV, are in both cases very large. They are about twice as large as the calculated values^{34,35} for *N,N'*-diphenyl-*N,N'*-bis(3-methylphenyl)-([1,1'-biphenyl])-4,4'-diamine (TPD), a

TABLE III. B3LYP/6-31G* relaxation energies (electronvolt) and intramolecular reorganization energies (electronvolt) for *PyPySPyPy* and *PPSPP*.

System	Neutral relaxation (λ_1) (eV)	Anionic relaxation (λ_2) (eV)	Total reorganization energy ($\lambda_1 + \lambda_2$) (eV)
<i>PyPySPyPy</i>	0.236	0.264	0.500
<i>PPSPP</i>	0.241	0.279	0.520

widely used hole-transport material, and four times as big as in pentacene.³⁶ This is directly related to the very strong geometrical changes occurring in the silole ring upon reduction.

From the energies of the optimized neutral and anionic structures, as well as single-point calculations of the neutral geometry on the anionic potential surface and the anionic geometry on the neutral potential surface, qualitative estimates of the electron affinity for *PyPySPyPy* and *PPSPP* can be made (note that the electron affinity is defined here as the energy of the neutral state subtracted from the energy of the radical-anion state; thus, a negative electron affinity reflects an energy stable radical-anion state). The adiabatic electron affinity for *PyPySPyPy* is -0.95 eV, while that for *PPSPP* is -0.75 eV. In comparison, the vertical electron affinity is -0.69 eV for *PyPySPyPy* and -0.47 eV for *PPSPP*. Both results qualitatively indicate a much more stable radical-anion state for *PyPySPyPy*.

It is worth noting that calculation of the dianionic state of both *PyPySPyPy* and *PPSPP* reveals significant energy destabilization versus the radical-anion and neutral states. For *PyPySPyPy*, the addition of a second electron to the stable radical-anion requires 2.12 eV; the dianion state is destabilized by 1.17 eV versus the neutral state. Formation of the dianion in *PPSPP* requires 2.31 eV, a state that is 1.56 eV less stable than the neutral state. The results for *PyPySPyPy* and *PPSPP* expose a significant divergence from the silole dianions theoretically studied by Goldfuss and von Ragué Schleyer,¹⁸ whereas silole rings that have undergone deprotonation of the hydrogen atoms present on the ring silicon allow for aromatic stabilization of the dianion, the presence of 1,1-dimethyl groups on the systems described herein do not permit such stabilization.

IV. CONCLUSIONS

While *PyPySPyPy* and *PPSPP* have been shown experimentally to display diverse solid-state electronic properties, the quantum-chemical analysis reported in this work indicates that the geometric and electronic structures, nature of the photoabsorption processes, and intramolecular reorganization energies are very similar for the two molecules. A direct answer as to why *PyPySPyPy* and *PPSPP* behave differently in the solid state cannot be easily provided based on the present study, since a deep understanding of the solid-state phenomena requires identification and appreciation of the effects of intermolecular interactions. Solid-state UPS and XPS investigations²⁴ have uncovered the formation of charge transfer complexes at the metal (Mg)-silole interface developed through strong chemical interactions, whereas charge hopping in the bulk silole film is probably best described through a polaron model. At this stage, one can only speculate that the more planar conformation found around the silole ring and the rings in the 2- and 5-positions in the case of *PyPySPyPy* might lead to stronger intermolecular interactions and tighter packing of these molecular segments. In general, such packing results in higher carrier mobilities and is conducive to luminescence quenching; an outcome in qualitative agreement with the comparison of the electron mobilities and photoluminescence quantum yields between

films of *PyPySPyPy* and *PPSPP*. Finally, we stress that, when considering electron transport, large reorganization energies on the order of 0.5 eV, are calculated for both *PyPySPyPy* and *PPSPP*. Such huge values, which are due to the significant extent and localized character of the geometry relaxation upon reduction, are detrimental to the achievement of high electron mobilities in the solid state.

ACKNOWLEDGMENTS

The authors would like to acknowledge the Office of Naval Research (ONR) for partial financial support. The work at Georgia Tech was partly supported by the National Science Foundation through the STC Program under Grant No. DMR-0120967 and through Grant No. CHE-0342321, ONR, and the IBM Shared University Research Program.

- ¹R. H. Friend, R. W. Gymer, A. B. Holmes *et al.*, *Nature* (London) **397**, 121 (1999).
- ²*Handbook of Conducting Polymers*, edited by T. A. Skotheim, R. L. Elsenbaumer, and J. R. Reynolds (Marcel Dekker, New York, 1998).
- ³Examples of the recent commercialization of organic light-emitting diode displays include: Kodak EasyShare LS633 Camera (http://www.kodak.com/eknec/PageQuerier.jhtml?pq-path=865&pq-locale=th_TH); Pioneer Organic EL Display CD (http://www.pioneerelectronics.com/pna/article/0,,2076_4035_48421,00.html); and, Philips Norelco 8894XL Spectra Shaving System (http://www.consumer.philips.com/global/b2c/norelco/catalog/product.jhtml?divId=NOR&groupId=DryRazors&subCatId=Spectra_2002&productId=8894XL_00).
- ⁴K. Tamao, M. Uchida, T. Izumizawa, K. Furukawa, and S. Yamaguchi, *J. Am. Chem. Soc.* **118**, 11974 (1996).
- ⁵S. Yamaguchi, Y. Itami, and K. Tamao, *Organometallics* **17**, 4910 (1998).
- ⁶H. Murata, G. G. Malliaras, M. Uchida, Y. Shen, and Z. H. Kafafi, *Chem. Phys. Lett.* **339**, 161 (2001).
- ⁷H. Murata, M. Uchida, and Z. H. Kafafi, *Appl. Phys. Lett.* **80**, 189 (2002).
- ⁸L. C. Palilis, A. J. Mäkinen, H. Murata, M. Uchida, and Z. H. Kafafi, *Organic Light-Emitting Materials and Devices VI*. Proceedings of SPIE-The International Society for Optical Engineering, edited by Z. H. Kafafi and H. Antoniadis (SPIE, Bellingham, WA, 2003), Vol. 4800, pp. 256–270.
- ⁹L. C. Palilis, H. Murata, A. J. Mäkinen, M. Uchida, and Z. H. Kafafi, *Org. Electron.* **4**, 113 (2003).
- ¹⁰J. Chen, C. W. Law, W. Y. Lam, Y. Dong, M. F. Low, I. D. Williams, D. Zhu, and Z. Tang, *Chem. Mater.* **15**, 1535 (2003).
- ¹¹L. C. Palilis, M. Uchida, and Z. H. Kafafi, *IEEE J. Sel. Top. Quantum Electron.* **10**, 79 (2004).
- ¹²A. D. Becke, *Phys. Rev. A* **38**, 3098 (1988); *J. Chem. Phys.* **98**, 5648 (1993).
- ¹³C. Lee, W. Yang, and R. G. Parr, *Phys. Rev. B* **37**, 785 (1988).
- ¹⁴J. C. Rienstra-Kiracofe, C. J. Barden, S. T. Brown, and H. F. Schaefer, *J. Phys. Chem. A* **105**, 524 (2001).
- ¹⁵J. C. Rienstra-Kiracofe, G. S. Tschumper, H. F. Schaefer, S. Nandi, and G. B. Ellison, *Chem. Rev. (Washington, D.C.)* **102**, 231 (2002).
- ¹⁶M. C. Zerner, G. H. Loew, R. F. Kichner, and U. T. Mueller-Westerhoff, *J. Am. Chem. Soc.* **102**, 589 (1980).
- ¹⁷M. J. Frisch *et al.*, GAUSSIAN 98, Revision A.11, Gaussian, Inc., Pittsburgh, PA, 2001.
- ¹⁸B. Goldfuss and P. von Ragué Schleyer, *Organometallics* **16**, 1543 (1997).
- ¹⁹V. N. Khabashesku, V. Balaji, S. E. Boganov, O. M. Nefedov, and J. Michl, *J. Am. Chem. Soc.* **116**, 320 (1994).
- ²⁰J. Ferman, J. P. Kakareka, W. T. Klooster *et al.*, *Inorg. Chem.* **38**, 2464 (1999).
- ²¹L. Párkányi, *J. Organomet. Chem.* **216**, 9 (1981).
- ²²M. Uchida, T. Izumizawa, T. Nakano, S. Yamaguchi, K. Tamao, and K. Furukawa, *Chem. Mater.* **13**, 2680 (2001).
- ²³A. J. Mäkinen, M. Uchida, and Z. H. Kafafi, *Appl. Phys. Lett.* **82**, 3889 (2003).
- ²⁴A. J. Mäkinen, M. Uchida, and Z. H. Kafafi, *J. Appl. Phys.* **95**, 2832 (2004).
- ²⁵The lowest-lying excited state geometry was optimized using coupled semiempirical RHF-AM1/configuration interaction (AM1/CI) as implemented in the AMPAC program package. AMPAC 5.0 Users Manual, Semi-chem (1994).
- ²⁶We adopt a nonantisymmetrized definition of the electron-hole distribution in analogy with S. Tretiak and S. Mukamel, *Chem. Rev. (Washington, D.C.)* **102**, 3171 (2002); J. Rissler, J. H. Bäessler, G. Gebhard, and P. Schwerdtfeger, *Phys. Rev. B* **64**, 045122 (2001).
- ²⁷S. Tretiak, A. Saxena, R. L. Martin, and A. R. Bishop, *Phys. Rev. Lett.* **89**, 097402 (2002).
- ²⁸R. J. Marcus, *J. Chem. Phys.* **24**, 966 (1956).
- ²⁹P. Barbara, T. Meyer, and M. Ratner, *J. Phys. Chem.* **100**, 13148 (1996).
- ³⁰J. Cornil, V. Lemaur, J. P. Calbert, and J. L. Brédas, *Adv. Mater.* **14**, 726 (2002).
- ³¹J. L. Brédas, J. P. Calbert, D. A. da Silva Filho, and J. Comil, *Proc. Natl. Acad. Sci. U.S.A.* **99**, 5804 (2002).
- ³²Y. C. Cheng, R. J. Silbey, D. A. da Silva Filho, J. P. Calbert, J. Comil, and J. L. Brédas, *J. Chem. Phys.* **118**, 3764 (2003).
- ³³V. Coropceanu, J. M. André, M. Malagoli, and J. L. Brédas, *Theor. Chem. Acc.* **110**, 59 (2003).
- ³⁴M. Malagoli and J. L. Brédas, *Chem. Phys. Lett.* **327**, 13 (2000).
- ³⁵B. C. Lin, C. P. Cheng, and Z. P. M. Lao, *J. Phys. Chem. A* **107**, 5241 (2003).
- ³⁶N. Gruhn, D. A. da Silva Filho, T. G. Bill, M. Malagoli, V. Coropceanu, A. Kahn, and J. L. Brédas, *J. Am. Chem. Soc.* **124**, 7918 (2002).